Same-sign Charged Higgs Pair Production in bosonic decay channels at the HL-LHC and HE-LHC

Chih-Ting Lu
(KIAS)

Collaborators :
Abdesslam Arhrib, Kingman Cheung
Ref : arXiv:1910.02571

The 1st Asian-European-Institutes (AEI) Workshop for BSM and the 9th KIAS Workshop on Particle Physics and Cosmology

Contents

- 1. Motivation
- 2. Brief review of 2HDM's
- 3. Constraints on 2HDM's
- 4. Same-sign charged Higgs pair production
- 5. Conclusions

Contents

Motivation : Incredible Success of the Standard Model

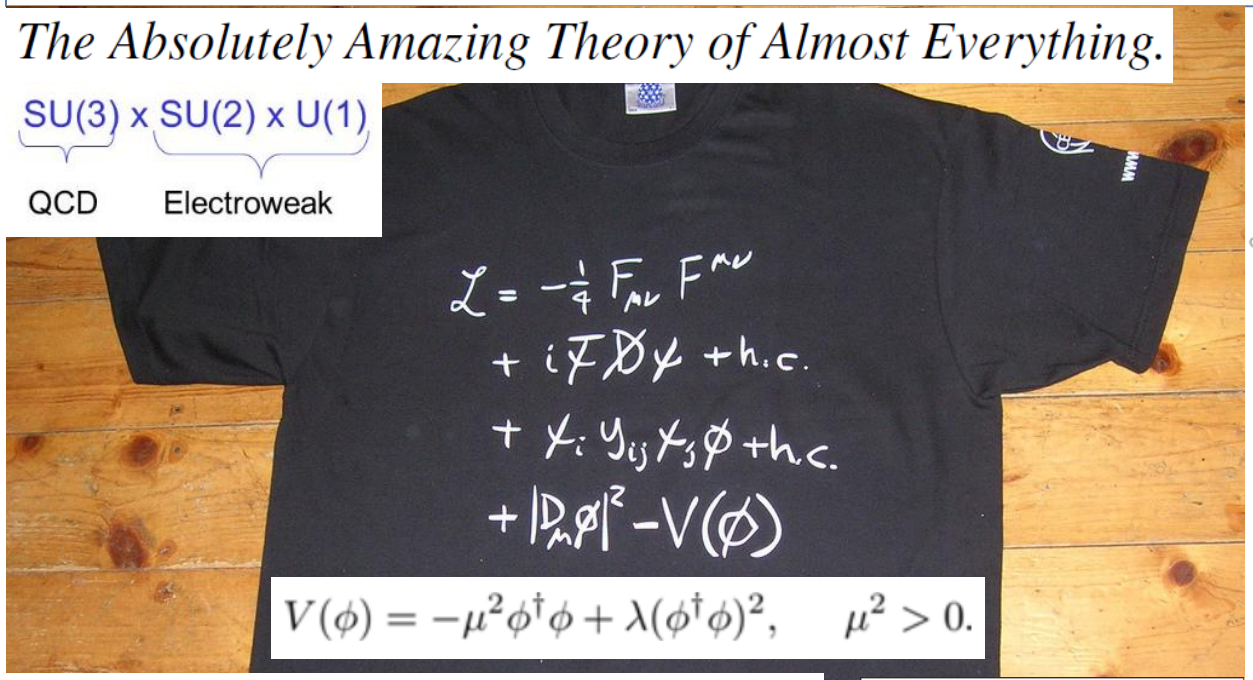

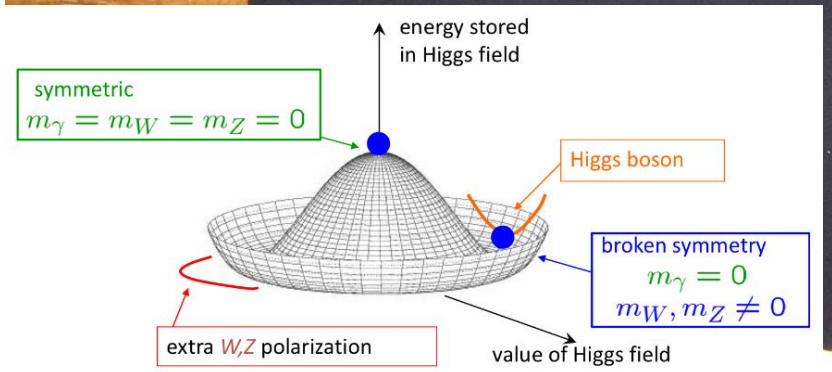

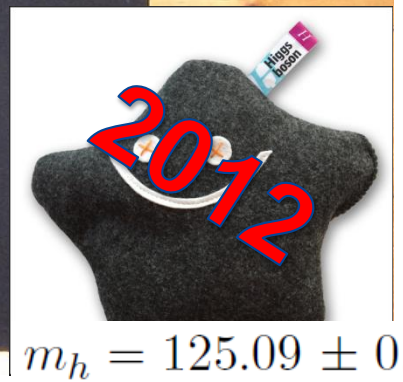

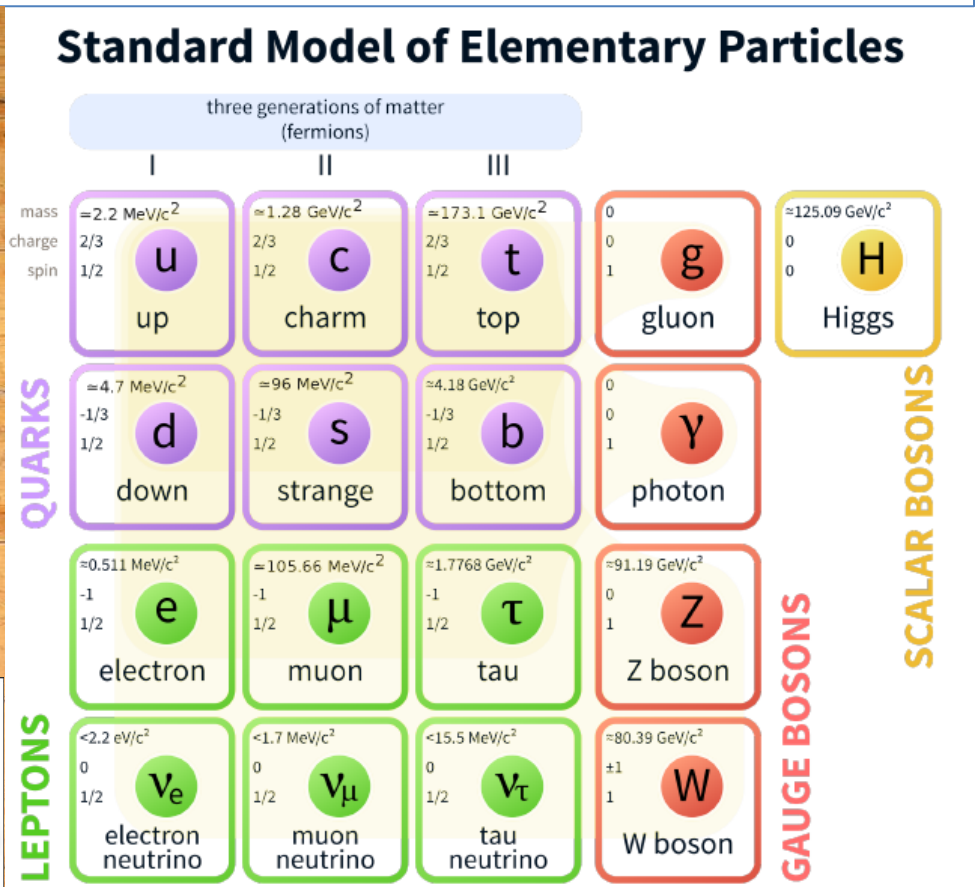

Fig. 1: Particle content of the Standard Model. Courtesy to Wikipedia.

$$m_h = 125.09 \pm 0.21\ (\text{stat.}) \pm 0.11\ (\text{syst.})\ \text{GeV}$$

The mission of the new LHC run at 14 TeV

- The first task is the improvement of the scalar boson mass and scalar boson coupling measurements.

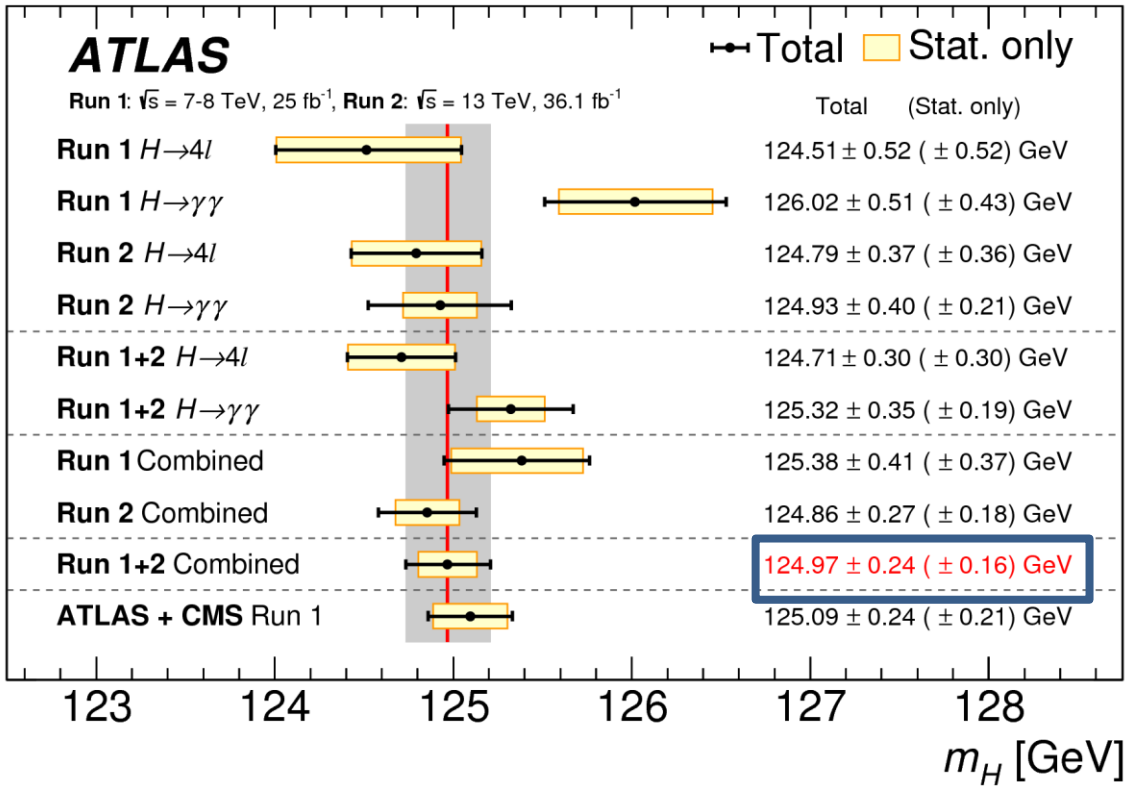

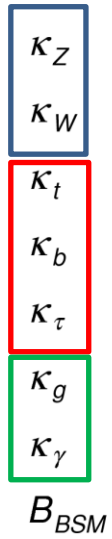

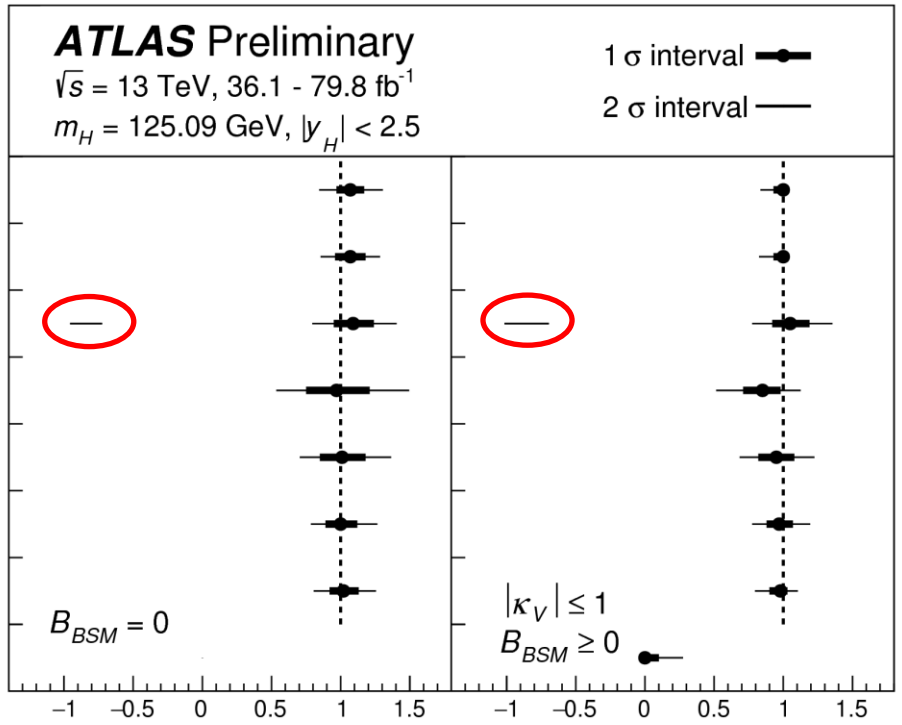

The mission of the new LHC run at 14 TeV

Accurate measurements of the scalar boson couplings to the SM particles would be helpful to determine if the Higgs-like particle is indeed the SM Higgs boson or a Higgs boson that belongs to a higher representation, such as models with extra Higgs doublets, extra triplets, or singlets.

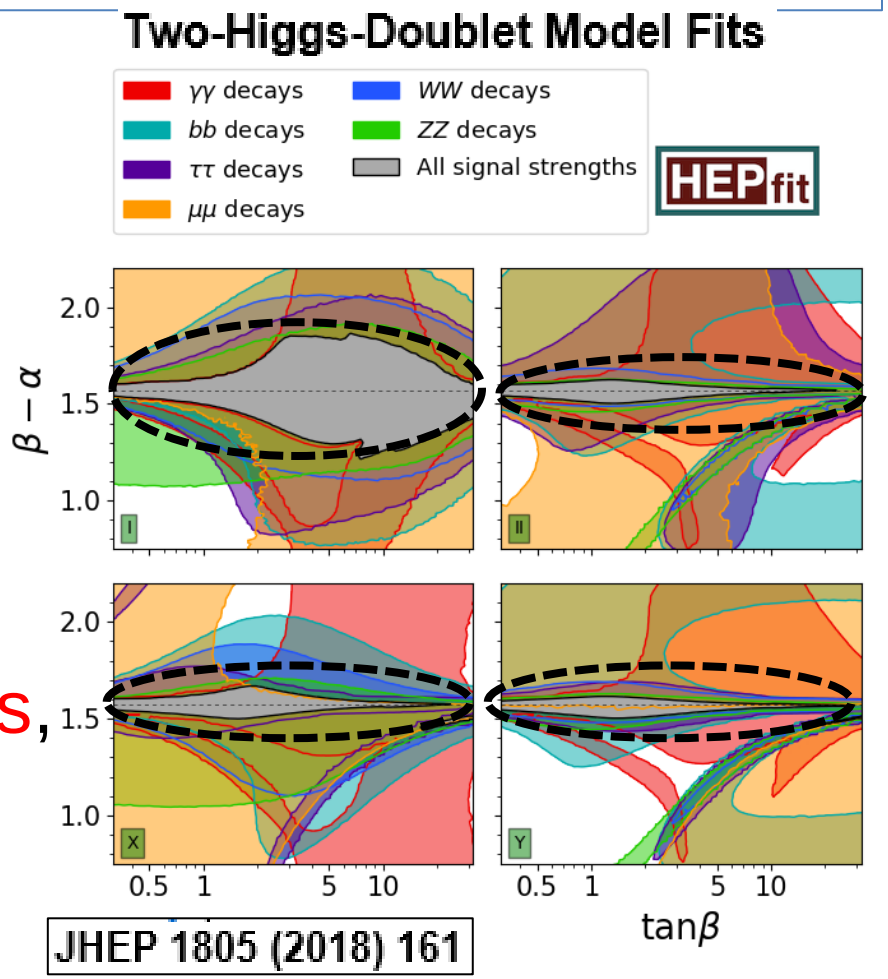

The mission of the new LHC run at 14 TeV

- The second task is to find a clear hint of new physics.
- Non-minimal Higgs sector models can explain the observed Higgs-like particle and account for some weakness of the SM.
- One common feature of many extensions of the presence of extra neutral Higgs bosons as well as singly-charged Higgs bosons in the physical spectrum.
- Therefore, the discovery of these extra bosons, especially for charged Higgs boson would be an unambiguous sign of physics beyond the SM.

Charged Higgs boson productions at hadron colliders

- 1. Production from top decay : $pp \to t\bar{t} \to t\bar{b}H^-$
- 2. Single charged Higgs production :
- (QCD processes : $gb \to tH^-$ & $gg \to t\bar{b}H^-$)
- (EW processes : $gg \to W^{\pm}H^{\mp}$, $b\bar{b} \to W^{\pm}H^{\mp}$ & $q\bar{q}' \to W^{\pm *} \to \phi H^{\pm}$)
- 3. Resonant charged Higgs production : $c\bar{s} \to H^+$, $c\bar{b} \to H^+$
- 4. Charged Higgs pair production through $q\bar{q}$ annihilation or gluon fusion.
- **5. Same-sign charged Higgs pair production :**

$$pp \to W^{\pm *}W^{\pm *}jj \to H^{\pm}H^{\pm}jj$$

Physics Letters B
Volume 797, 10 October 2019, 134854

Masashi Aiko, Shinya Kanemura, Kentarou Mawatari (Osaka U.)

arXiv:1906.09101

Same-sign charged Higgs pair production

- 1. The full process : $pp \to W^{\pm *} W^{\pm *} \to jj H^{\pm} H^{\pm} \to jj (W^{\pm} A^0)(W^{\pm} A^0)$
- 2. The production cross section scales as the square of the mass difference $\Delta m = (m_{H^0} - m_{A^0})$ in the alignment limit $(\cos(\beta - \alpha) = 0)$
- 3. We focus on light pseudoscalar and large mass difference with
- $m_{A^0} = 30 - 100 \text{ GeV}$, $\Delta m \equiv m_{H^0} - m_{A^0} = 200 - 250 \text{ GeV}$
- in Type-I and III 2HDM's.

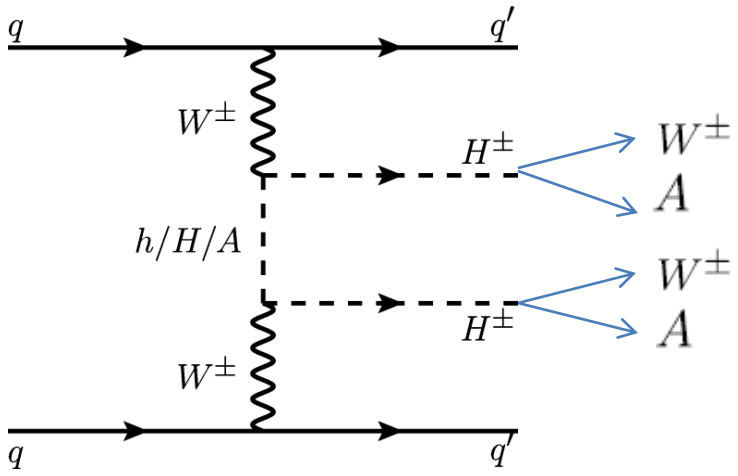

Contents

- 1. Motivation
- **2. Brief review of 2HDM's**
- 3. Constraints on 2HDM's
- 4. Same-sign charged Higgs pair production
- 5. Conclusions

Brief review of 2HDMs

In the two-Higgs-Doublet Model (2HDM), two Higgs doublet fields $\Phi_{1,2}$ with hypercharge $Y_{\Phi_{1,2}} = 1/2$ are introduced. The most general renormalizable scalar potential, which respects the $SU_L(2) \otimes U_Y(1)$ gauge symmetry, has the following form:

$$\begin{aligned} V(\Phi_1, \Phi_2) = & \, m_{11}^2 \, \Phi_1^\dagger \Phi_1 + m_{22}^2 \, \Phi_2^\dagger \Phi_2 + m_{12}^2 \, \left(\Phi_1^\dagger \Phi_2 + \Phi_2^\dagger \Phi_1 \right) + \frac{\lambda_1}{2} \left(\Phi_1^\dagger \Phi_1 \right)^2 + \frac{\lambda_2}{2} \left(\Phi_2^\dagger \Phi_2 \right)^2 \\ & + \lambda_3 \, \Phi_1^\dagger \Phi_1 \, \Phi_2^\dagger \Phi_2 + \lambda_4 \, \Phi_1^\dagger \Phi_2 \, \Phi_2^\dagger \Phi_1 + \frac{\lambda_5}{2} \left[\left(\Phi_1^\dagger \Phi_2 \right)^2 + \left(\Phi_2^\dagger \Phi_1 \right)^2 \right] \end{aligned} \tag{2}$$

where m_{11}^2, m_{22}^2 and $\lambda_{1,2,3,4}$ are real, while m_{12}^2 and λ_5 could be complex for CP violation purpose.

Brief review of 2HDMs

Assuming that both Φ_1 and Φ_2 acquire a vacuum expectation value (VEV) $v_{1,2}$ that can induce electroweak symmetry breaking, the two complex scalar $SU_L(2)$ doublets can be decomposed according to

$$\Phi_i = \begin{pmatrix} \phi_i^+ \\ (v_i + \rho_i + i\eta_i)/\sqrt{2} \end{pmatrix}, \quad i = 1, 2\,. \tag{3}$$

The mass eigenstates for the Higgs sector are obtained by orthogonal transformations,

$$\begin{pmatrix} \phi_1^\pm \\ \phi_2^\pm \end{pmatrix} = R_\beta \begin{pmatrix} G^\pm \\ H^\pm \end{pmatrix}, \quad \begin{pmatrix} \rho_1 \\ \rho_2 \end{pmatrix} = R_\alpha \begin{pmatrix} H^0 \\ h^0 \end{pmatrix}, \quad \begin{pmatrix} \eta_1 \\ \eta_2 \end{pmatrix} = R_\beta \begin{pmatrix} G^0 \\ A^0 \end{pmatrix},$$

with the generic form $(\theta = \alpha, \beta)$

$$R_\theta = \begin{pmatrix} \cos\theta & -\sin\theta \\ \sin\theta & \cos\theta \end{pmatrix}. \qquad \tan\beta \equiv v_2/v_1$$

Brief review of 2HDMs

We are then left with seven independent parameters which can be taken as:

the four physical masses m_h, m_H, m_A and $m_{H\pm}$, CP-even mixing angle α, $\tan\beta$ and m_{12}^2.

In order to avoid Flavor-Changing Neutral Current (FCNC), a discrete symmetry Z_2 (where for example $\Phi_1 \to \Phi_1$ and $\Phi_2 \to -\Phi_2$) is imposed

The most general Yukawa interaction can be written as follows

$$-\mathcal{L}_{\text{Yukawa}}^{\text{2HDM}} = \overline{Q}_L Y_u \widetilde{\Phi}_2 u_R + \overline{Q}_L Y_d \Phi_d d_R + \overline{L}_L Y_\ell \Phi_\ell \ell_R + \text{h.c},$$

where $\Phi_{d,l}$ $(d, l = 1, 2)$ represent Φ_1 or Φ_2, Y_f $(f = u, d \text{ or } \ell)$ stand for 3×3 Yukawa matrices and $\widetilde{\Phi}_2 = i\sigma_2 \Phi_2^\star$.

Brief review of 2HDMs

$$-\mathcal{L}_{\text{Yukawa}}^{\text{2HDM}} = \sum_{f=u,d,\ell} \frac{m_f}{v}\left(\xi_f^{h^0}\overline{f}fh^0 + \xi_f^{H^0}\overline{f}fH^0 - i\xi_f^{A^0}\overline{f}\gamma_5 fA^0\right)$$
$$+\left\{\frac{\sqrt{2}V_{ud}}{v}\,\overline{u}\left(m_u\xi_u^{A^0}\mathrm{P}_L + m_d\xi_d^{A^0}\mathrm{P}_R\right)dH^+ + \frac{\sqrt{2}m_\ell\xi_\ell^{A^0}}{v}\,\overline{\nu_L}\ell_R H^+ + \text{h.c}\right\}$$

Model	u_R^i	d_R^i	e_R^i
Type I	Φ_2	Φ_2	Φ_2
Type II	Φ_2	Φ_1	Φ_1
Lepton-specific	Φ_2	Φ_2	Φ_1
Flipped	Φ_2	Φ_1	Φ_2

type	$\xi_u^{A^0}$	$\xi_d^{A^0}$	$\xi_l^{A^0}$
I	$\cot\beta$	$-\cot\beta$	$-\cot\beta$
II	$\cot\beta$	$\tan\beta$	$\tan\beta$
III	$\cot\beta$	$-\cot\beta$	$\tan\beta$
IV	$\cot\beta$	$\tan\beta$	$-\cot\beta$

Contents

- 1. Motivation
- 2. Brief review of 2HDM's
- **3. Constraints on 2HDM's**
- 4. Same-sign charged Higgs pair production
- 5. Conclusions

Constraints on 2HDM's

Theoretical constraints :

(1) All set of tree-level perturbative unitarity conditions

(2) All λ_i's remain perturbative

(3) The potential remains bounded from below,

$$\lambda_1 > 0 \ , \ \lambda_2 > 2 \ , \ \sqrt{\lambda_1 \lambda_2} + \lambda_3 + \min(0, \lambda_4 + \lambda_5, \lambda_4 - \lambda_5)$$

Experimental constraints from indirect searches :

(1) Electro-Weak Precision Observable (EWPOs)

(2) Flavor physics

Electro-Weak Precision Observable (EWPOs)

- The EWPOs can be represented by a set of oblique parameters S, T and U.
- We emphasize that the T parameter, which is related to the amount of isospin violation, is sensitive to the mass splitting among $H^{\pm}$, H^0, and A^0.
- From 2018 PDG review with fixed U=0, the best fit of S, T parameters can be represented as

$$S = 0.02 \pm 0.07 \qquad T = 0.06 \pm 0.06$$

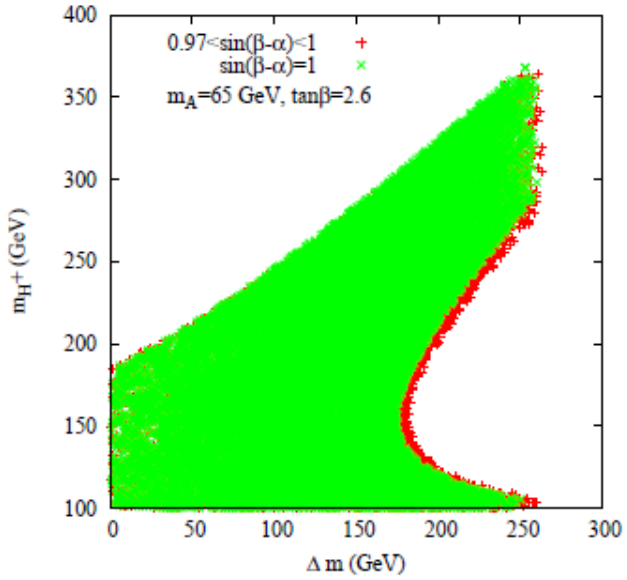
0.97<sin(β-α)<1
sin(β-α)=1
m_A=65 GeV, tanβ=2.6
m_H+ (GeV)
Δ m (GeV)

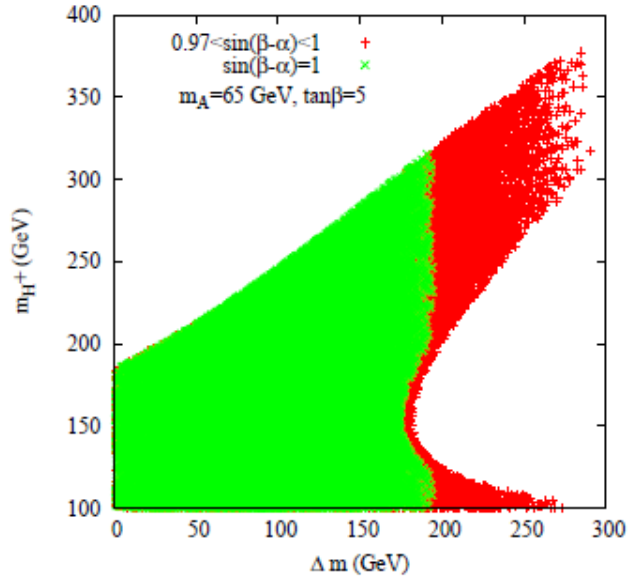
0.97<sin(β-α)<1
sin(β-α)=1
m_A=65 GeV, tanβ=5
m_H+ (GeV)
Δ m (GeV)

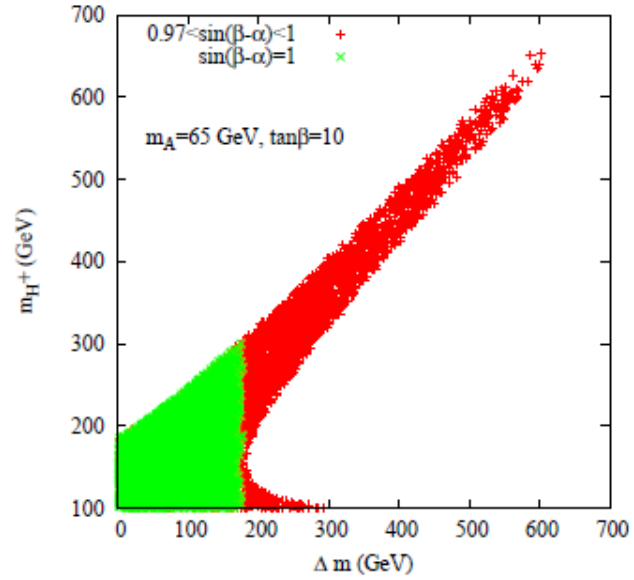
0.97<sin(β-α)<1
sin(β-α)=1
m_A=65 GeV, tanβ=10
m_H+ (GeV)
Δ m (GeV)

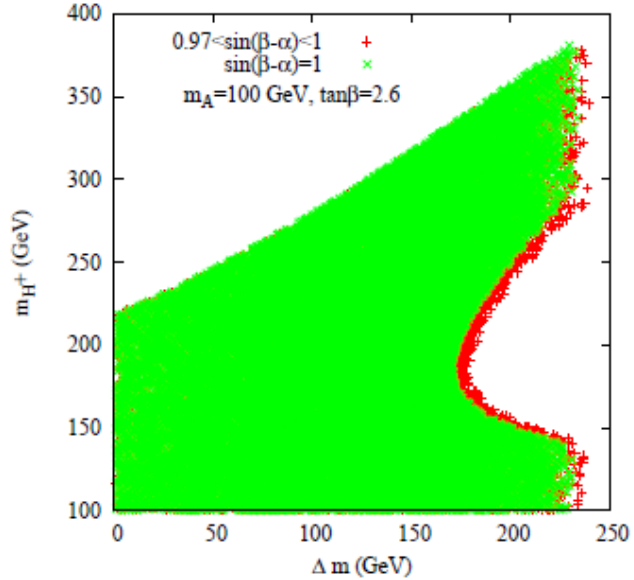
0.97<sin(β-α)<1
sin(β-α)=1
m_A=100 GeV, tanβ=2.6
m_H+ (GeV)
Δ m (GeV)

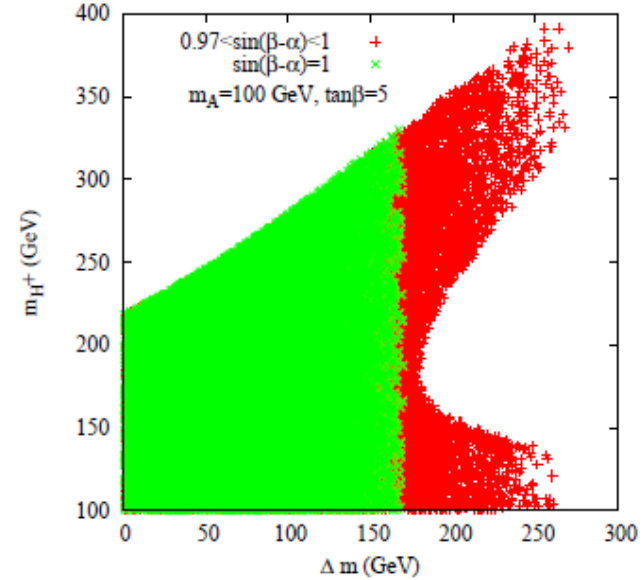
0.97<sin(β-α)<1
sin(β-α)=1
m_A=100 GeV, tanβ=5
m_H+ (GeV)
Δ m (GeV)

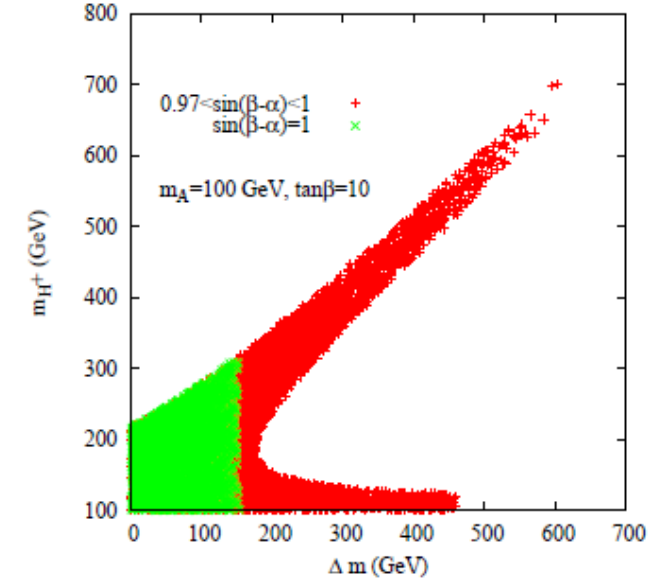
0.97<sin(β-α)<1
sin(β-α)=1
m_A=100 GeV, tanβ=10
m_H+ (GeV)
Δ m (GeV)

B physics constraints

The most severe constraints in flavor physics are due to the measurements of $B(B \to X_s\gamma)$, $B(B_{d,s} \to \mu^+\mu^-)$ and Δm_s of B mesons. For $B(B \to X_s\gamma)$, according to the latest analysis by [30], we have:

- In 2HDM type-II and IV, the $b \to s\gamma$ constraint forces the charged Higgs mass to be heavier than 580 GeV [30, 31] for any value of $\tan\beta \geq 1$.
- In 2HDM-I and III, charged Higgs with mass as low as $\sim 100 - 200$ GeV [30, 32] is still allowed as long as $\tan\beta \geq 2$.

For other B-physics observables we refer to the recent analysis [33], in which they also included Δm_s and $B_{d,s} \to \mu^+\mu^-$. For a light charged Higgs boson, $100 < m_{H^\pm} < 200$ GeV, of interest in this study, one can conclude from [33] that $\tan\beta \geq 3$ is allowed for 2HDM type I and III.

$H^{\pm}$ and A^0 branching ratios and Direct searches

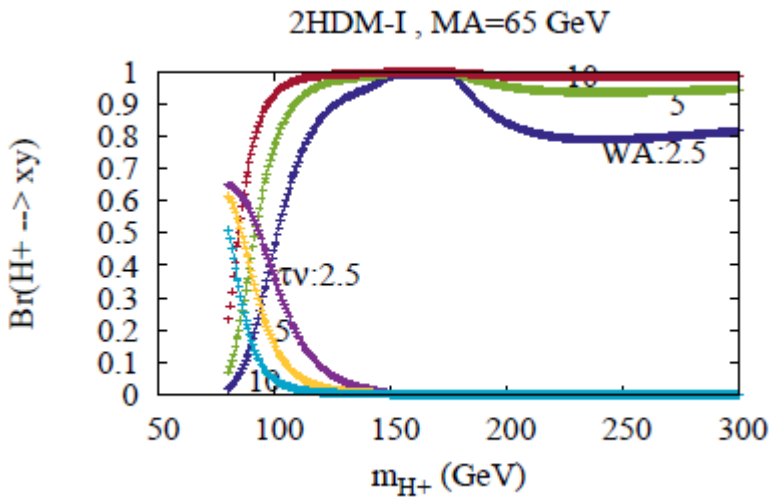

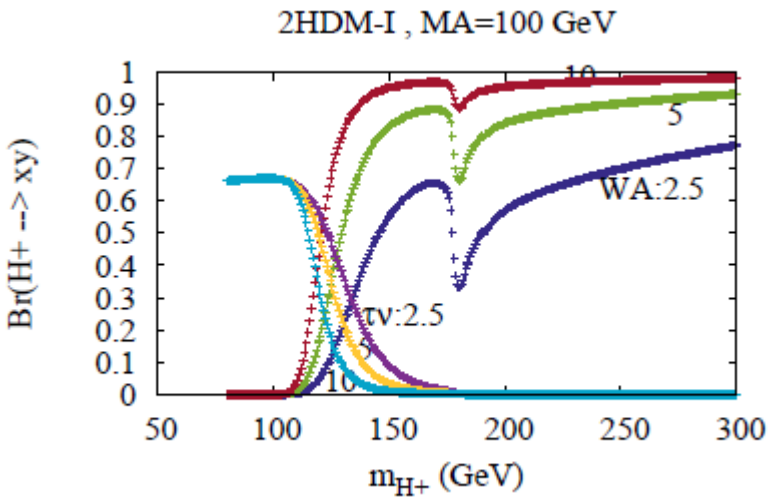

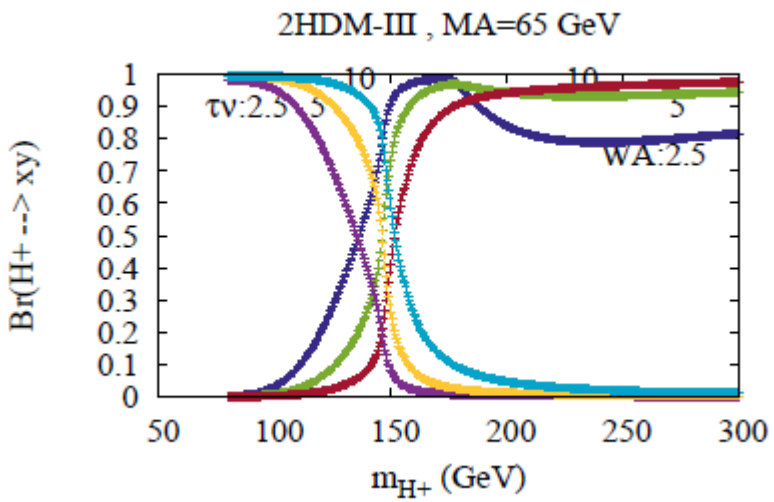

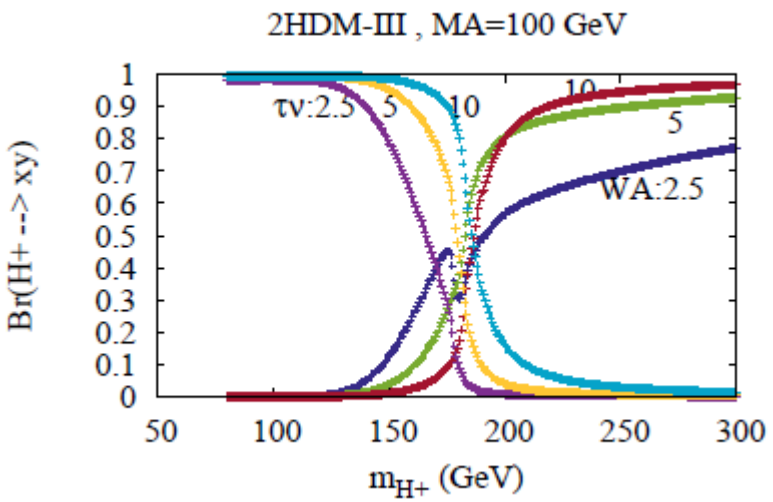

$H^{\pm}$ and A^0 branching ratios and Direct searches

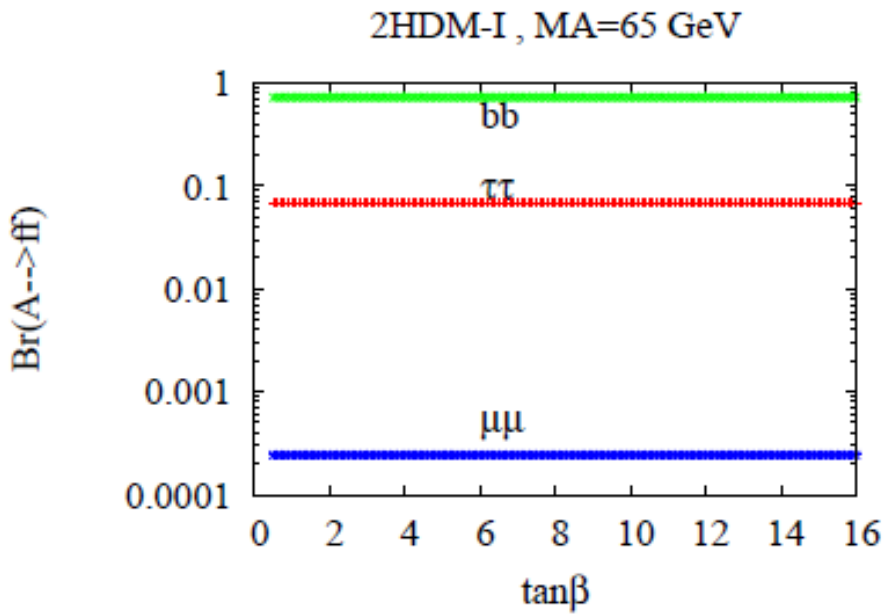

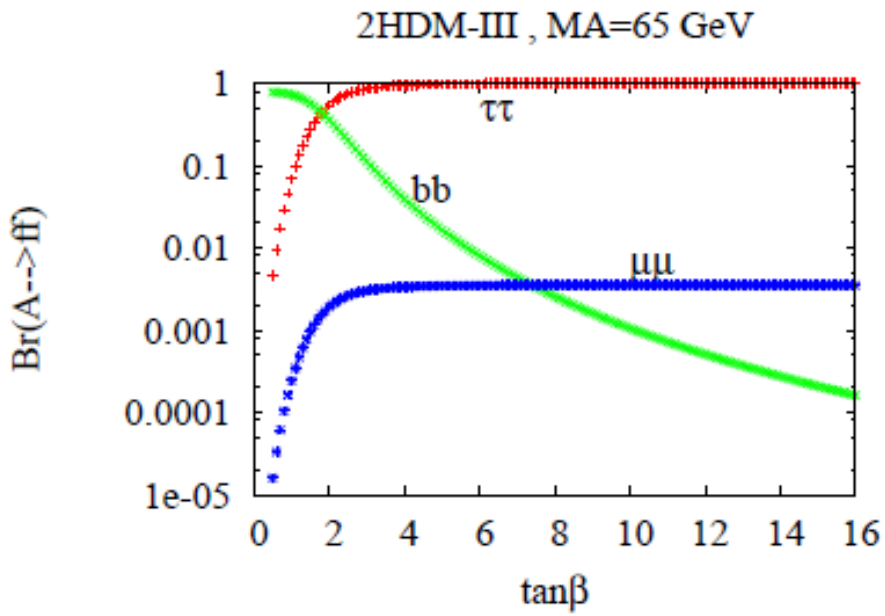

$LHC\ Constraint\ from\ t \to bH^+ \to b\tau\nu_\tau$

CMS Collaboration JHEP 07 (2019) 142 arXiv:1903.04560

Search for charged Higgs bosons in the $H^\pm \to \tau^\pm \nu_\tau$ decay channel in proton-proton collisions at $\sqrt{s} = 13$ TeV

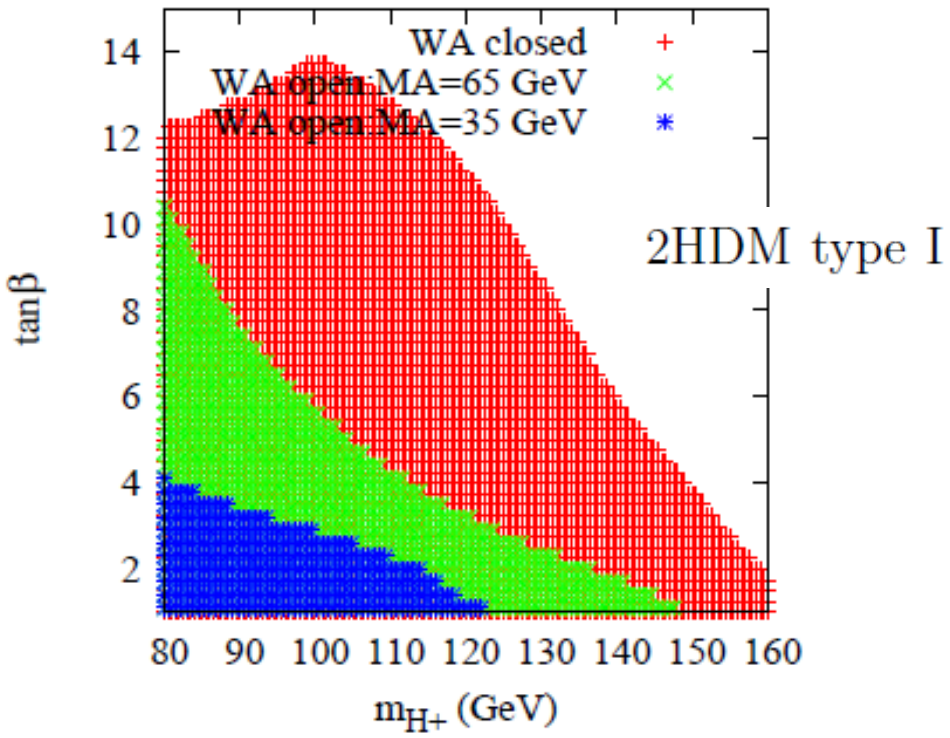

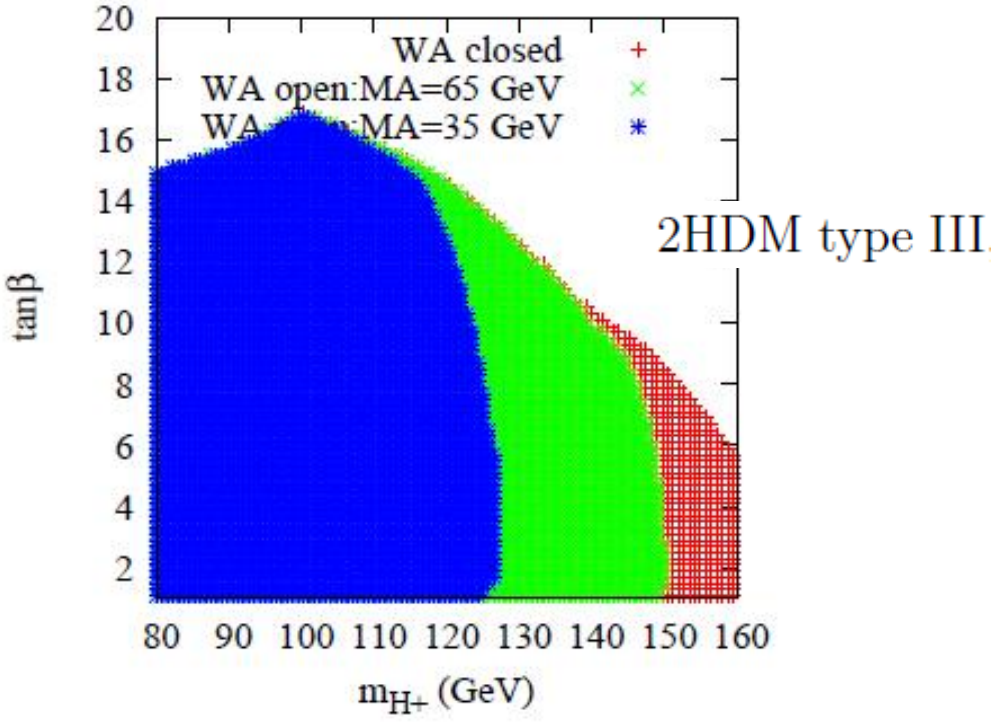

$LHC\ Constraint\ from\ t \to bH^+ \to bA^0W^+ \to bW^+\mu^+\mu^-$

CMS Collaboration Phys. Rev. Lett. 123, 131802 (2019) arXiv:1905.07453

Search for a light charged Higgs boson decaying to a W boson and a CP-odd Higgs boson in final states with e$\mu\mu$ or $\mu\mu\mu$ in proton-proton collisions at $\sqrt{s} = 13$ TeV

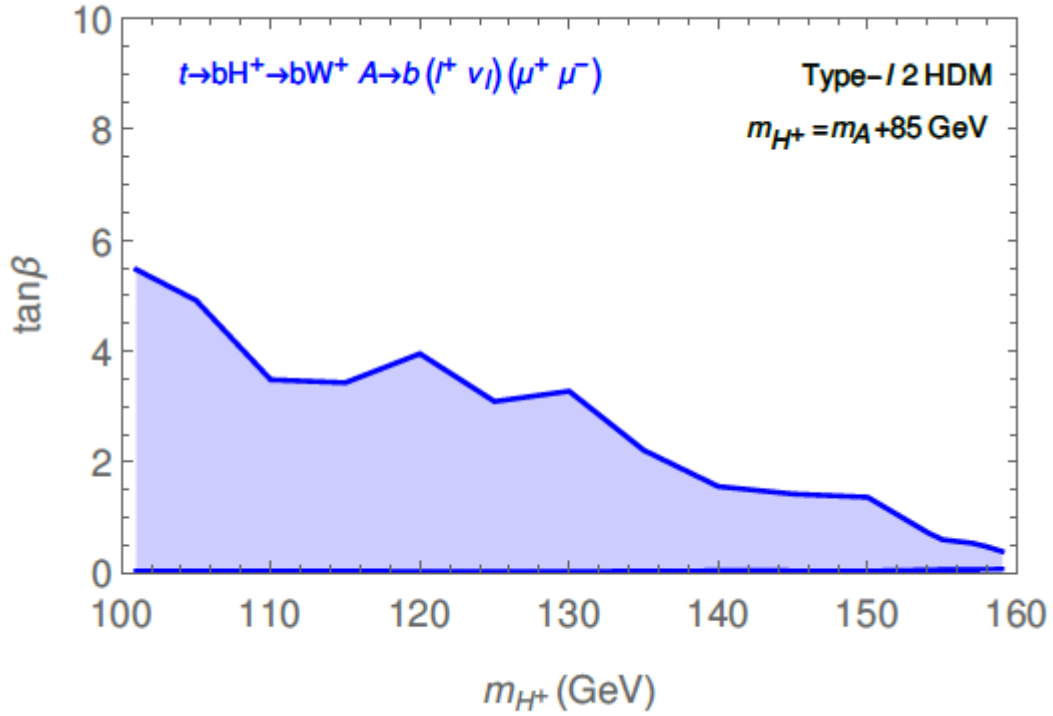

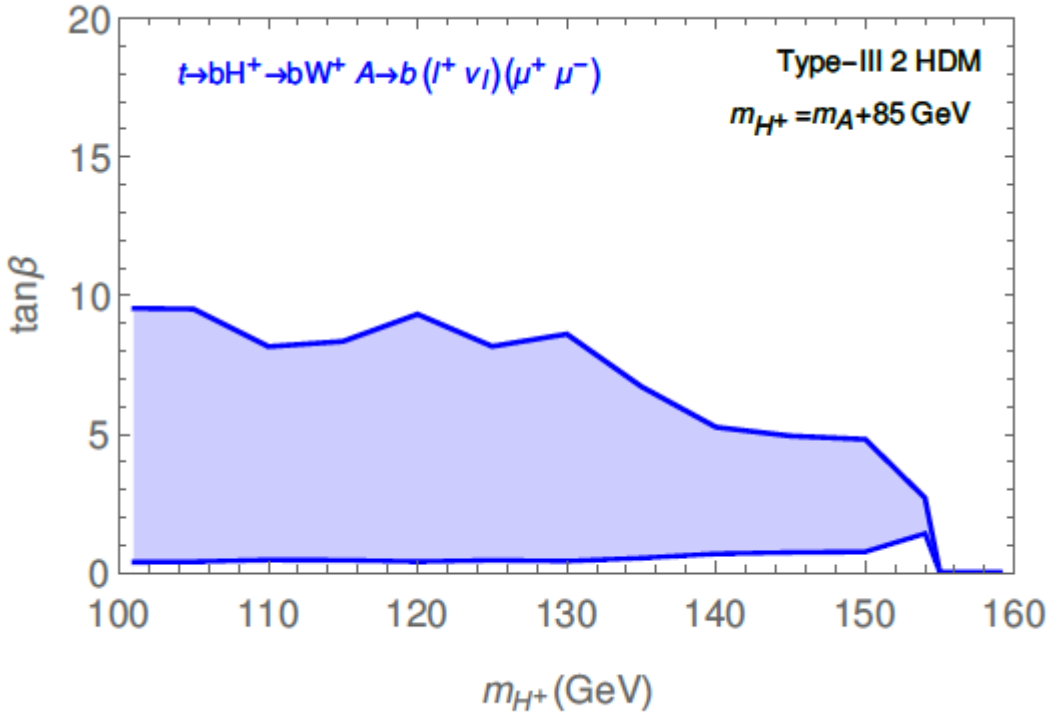

Contents

- 1. Motivation
- 2. Brief review of 2HDM's
- 3. Constraints on 2HDM's
- **4. Same-sign charged Higgs pair production**
- 5. Conclusions

The behavior of $pp \to H^{\pm}H^{\pm}j_F j_F$ process

The relation between the mass splitting Δm and same-sign charged Higgs pair production can be understood in the $2 \to 2$ subprocess $W^+W^+ \to H^+H^+$ at amplitude level. This subprocess is induced by three t-channel diagrams with h^0, H^0 and A^0 exchange. In the alignment limit, $\cos(\beta - \alpha) = 0$, which is favored by the current Higgs data, the scattering amplitude for

$$W^+(p_1)W^+(p_2) \to H^+(q_1)H^+(q_2)$$

is only mediated by H^0 and A^0 and is given by

$$i\mathcal{M}^{H^0+A^0} = ig^2 q_1 \cdot \epsilon(p_1)\, q_2 \cdot \epsilon(p_2) \left[\frac{1}{t - m^2_{A^0}} - \frac{1}{t - m^2_{H^0}}\right] + (q_1 \leftrightarrow q_2, t \leftrightarrow u) \qquad (9)$$

where $t = (p_1 - q_1)^2$ and $u = (p_1 - q_2)^2$, and $\epsilon(p_{1,2})$ are the polarization 4-vector of the incoming W^+ bosons. In the approximation $m_{A^0} \approx m_{H^0}$, the amplitude reduces to

$$i\mathcal{M}^{H^0+A^0} = -ig^2 q_1 \cdot \epsilon(p_1)\, q_2 \cdot \epsilon(p_2)\, \frac{2m_{A^0}}{(t - m^2_{A^0})^2} \Delta m + (q_1 \leftrightarrow q_2, t \leftrightarrow u) \qquad (10)$$

It is clear to see that the amplitude is proportional to Δm from the above formula with $m_{A^0} \approx m_{H^0}$.

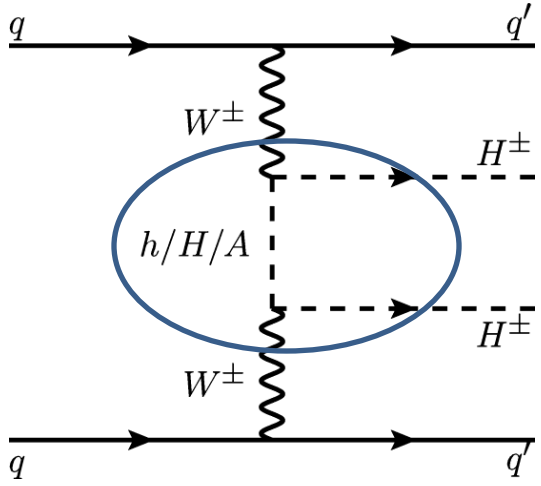

The behavior of $pp \to H^{\pm}H^{\pm}j_F j_F$ process

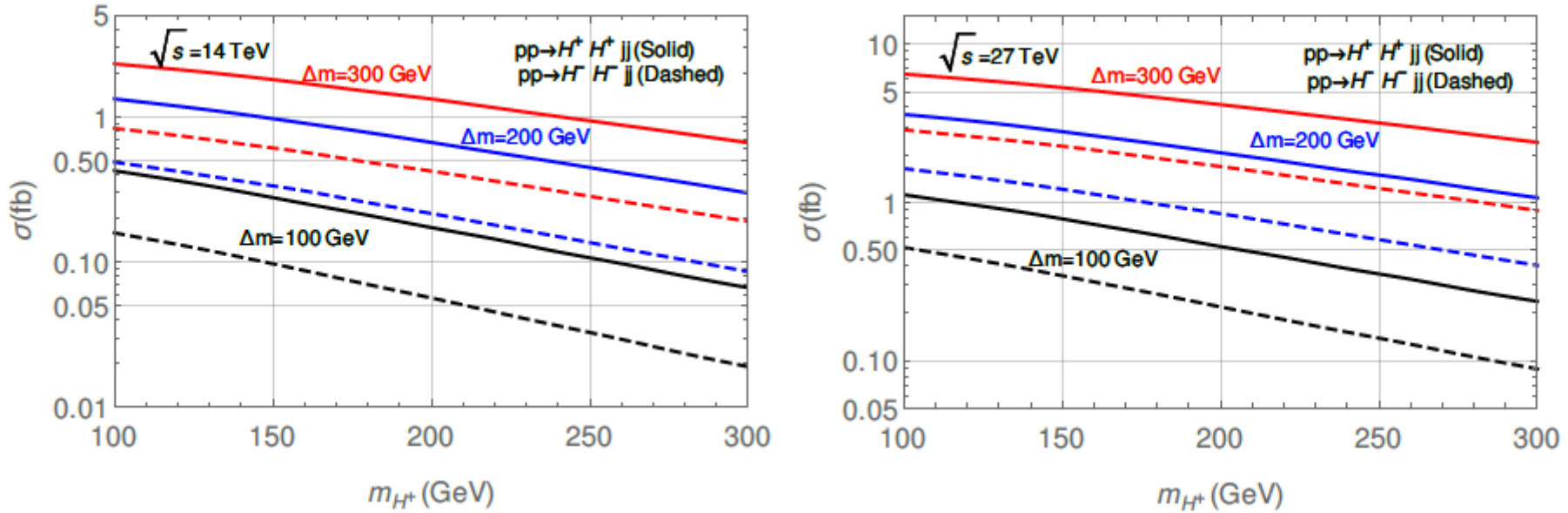

alignment limit $(\cos(\beta - \alpha) = 0)$

FIG. 6. The production cross sections of $pp \to H^+H^+j_F j_F$ (solid line) and $pp \to H^-H^-j_F j_F$ (dashed line) versus $m_{H^\pm}$ at $\sqrt{s} = 14$ TeV (left panel) and $\sqrt{s} = 27$ TeV (right panel), for Δm =100 GeV (black), 200 GeV (blue), and 300 GeV (red). Notice the VBF cut $\eta_{j_1} \times \eta_{j_2} < 0$ and $|\Delta\eta_{jj}| > 2.5$ for the minimum rapidity difference between the forward jet pair are applied.

Signal-background analysis for Type-I 2HDM

- The signal process

$$pp \to W^{\pm *}W^{\pm *}j_F j_F \to H^{\pm}H^{\pm}j_F j_F \to (W^{\pm}A^0)(W^{\pm}A^0)j_F j_F \to l^{\pm}\nu(b\bar{b})l^{\pm}\nu(b\bar{b})j_F j_F$$

- The main SM backgrounds

$$pp \to t\bar{t}t\bar{t} \to (bW^+)(\bar{b}W^-)(bW^+)(\bar{b}W^-) \to l^{\pm}l^{\pm}4b4j,$$

$$pp \to t\bar{b}\bar{t}bl^+l^- \to (bW^+)\bar{b}(\bar{b}W^-)bl^+l^- \to l^{\pm}l^+l^-4b2j,$$

$$pp \to t\bar{t}t\bar{b} \to (bW^+)(\bar{b}W^-)(bW^+)\bar{b} \to l^+l^+4b2j$$

$$or \quad pp \to t\bar{t}tb \to (bW^+)(\bar{b}W^-)(\bar{b}W^-)b \to l^-l^-4b2j,$$

$$pp \to tt\bar{b}\bar{b}jj \to (bW^+)(bW^+)\bar{b}\bar{b}jj \to l^+l^+4b2j$$

$$or \quad pp \to \bar{t}\bar{t}bbjj \to (\bar{b}W^-)(\bar{b}W^-)bbjj \to l^-l^-4b2j\,.$$

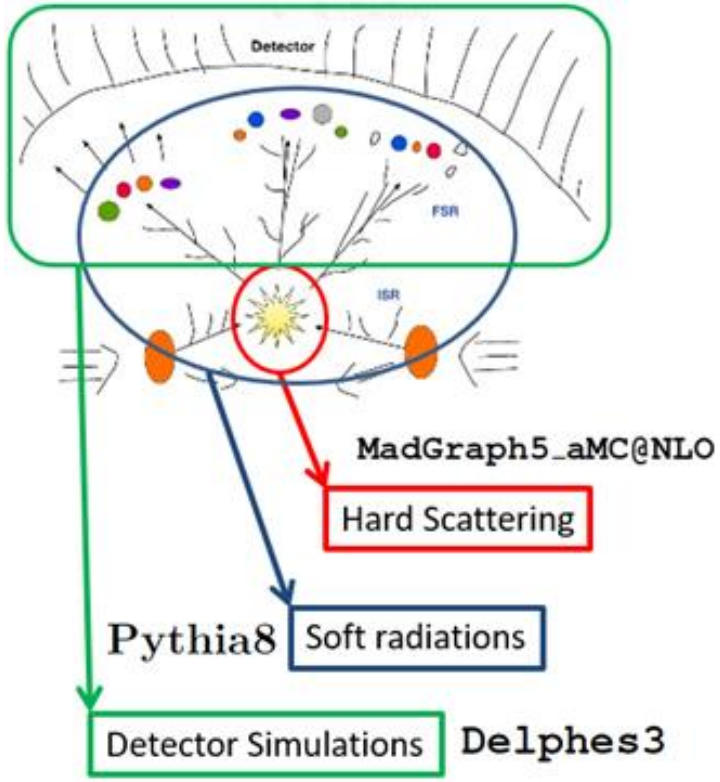

Signal-background analysis for Type-I 2HDM

TABLE IV. Cut flow table for the Type-I 2HDM signal $pp \to H^{\pm}H^{\pm}j_F j_F$ with $m_{H^{\pm}} = 205$ GeV, $m_{A^0} = 65$ GeV, $\Delta m = 200$ GeV, $\tan\beta = 5$ and $\sin(\beta-\alpha) = 0.97$, and various backgrounds at $\sqrt{s} = 14$ TeV.

MadAnalysis5

Cross section (fb)	signal	$t\bar{t}t\bar{t}$	$t\bar{t}b\bar{b}l^+l^-$	$3t1b$	$2t2b2j$
Preselection	2.07×10^{-2}	4.94×10^{-2}	1.08×10^{-2}	7.74×10^{-5}	8.29×10^{-5}
$N(b, l^{\pm}) \geq 3, 2$, $P_T^{b,l^{\pm}} > 20$GeV, $\lvert\eta^{b,l}\rvert < 2.5$	1.76×10^{-3}	6.17×10^{-3}	9.56×10^{-4}	9.57×10^{-6}	9.81×10^{-6}
$N(j) \geq 2$, $P_T^j > 30$GeV, $M_{jj} > 500$GeV	1.46×10^{-3}	5.15×10^{-3}	4.18×10^{-4}	2.88×10^{-6}	4.05×10^{-6}
$m_{H^{\pm}}$ Cuts					
$M_{bbl^{\pm}} < 250$GeV	1.41×10^{-3}	3.50×10^{-3}	2.71×10^{-4}	1.85×10^{-6}	2.62×10^{-6}
m_A Cuts					
$50 < M_{bb} < 90$GeV	1.30×10^{-3}	1.68×10^{-3}	1.61×10^{-4}	7.58×10^{-7}	1.14×10^{-6}

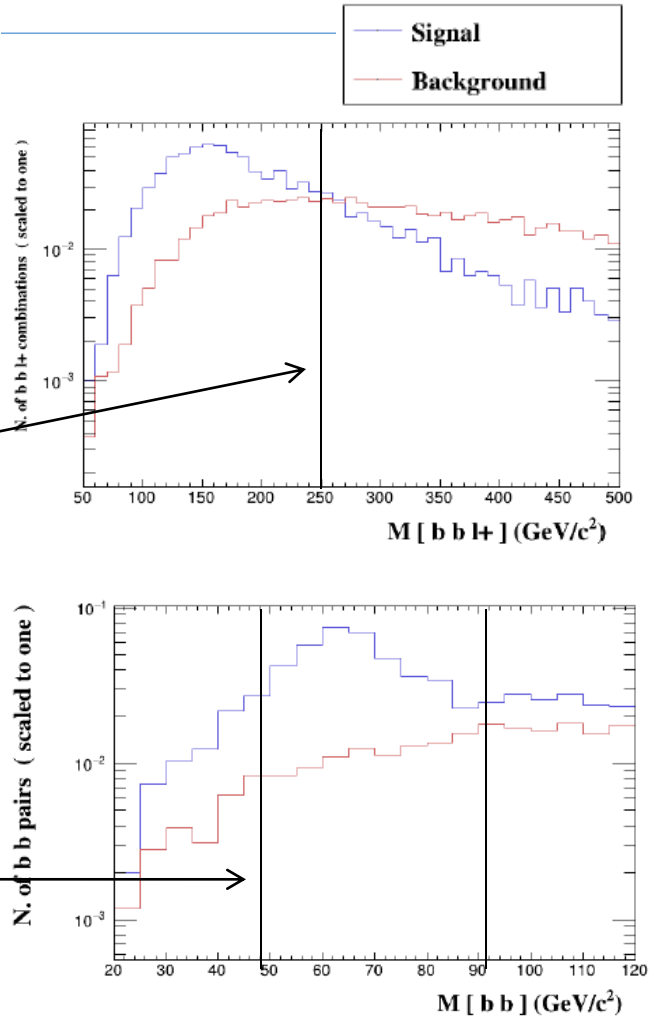

Signal-background analysis for Type-I 2HDM

TABLE V. Cut flow table for the Type-I 2HDM signal $pp \to H^{\pm}H^{\pm}j_F j_F$ with $m_{H^{\pm}} = 205$ GeV, $m_{A^0} = 65$ GeV, $\Delta m = 200$ GeV, $\tan\beta = 5$ and $\sin(\beta - \alpha) = 0.97$, and various backgrounds at $\sqrt{s} = 27$ TeV.

MadAnalysis5

Cross section (fb)	signal	$t\bar{t}t\bar{t}$	$t\bar{t}b\bar{b}l^+l^-$	$3t1b$	$2t2b2j$
Preselection	6.88×10^{-2}	5.67×10^{-1}	5.60×10^{-2}	2.40×10^{-4}	6.76×10^{-4}
$N(b, l^{\pm}) \geq 3, 2,$ $P_T^{b,l^{\pm}} > 20\text{GeV}, \lvert\eta^{b,l}\rvert < 2.5$	5.15×10^{-3}	5.67×10^{-2}	4.43×10^{-3}	2.44×10^{-5}	6.42×10^{-5}
$N(j) \geq 2,$ $P_T^j > 30\text{GeV}, M_{jj} > 500\text{GeV}$	4.54×10^{-3}	5.22×10^{-2}	2.49×10^{-3}	9.67×10^{-6}	3.27×10^{-5}
$m_{H^{\pm}}$ Cuts $M_{bbl^{\pm}} < 200\text{GeV}$	4.10×10^{-3}	2.28×10^{-2}	1.08×10^{-3}	4.29×10^{-6}	1.45×10^{-5}
m_A Cuts $50 < M_{bb} < 80\text{GeV}$	3.76×10^{-3}	1.12×10^{-2}	6.09×10^{-4}	1.91×10^{-6}	7.15×10^{-6}

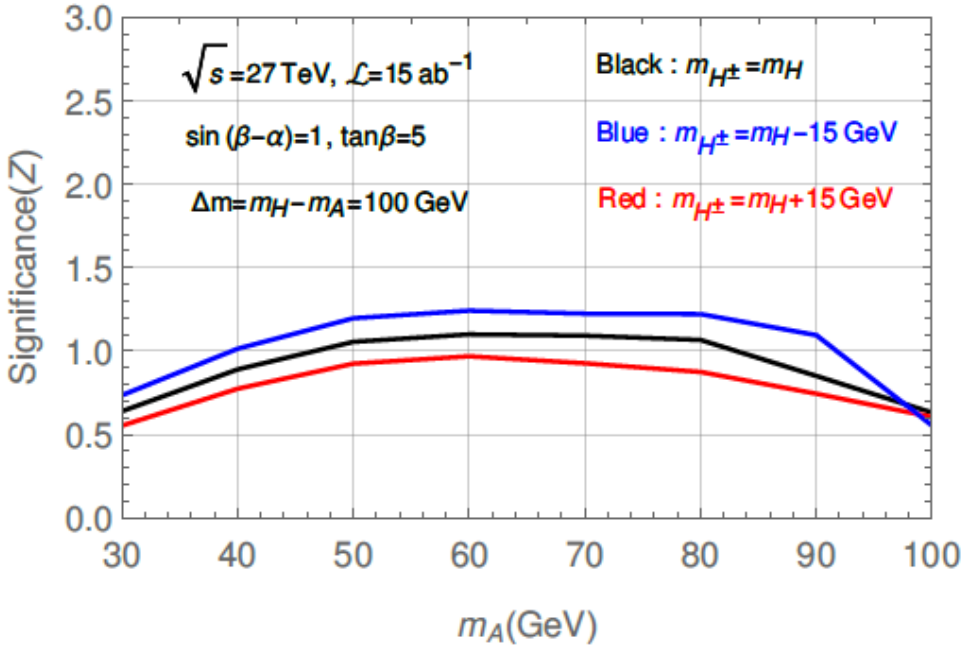

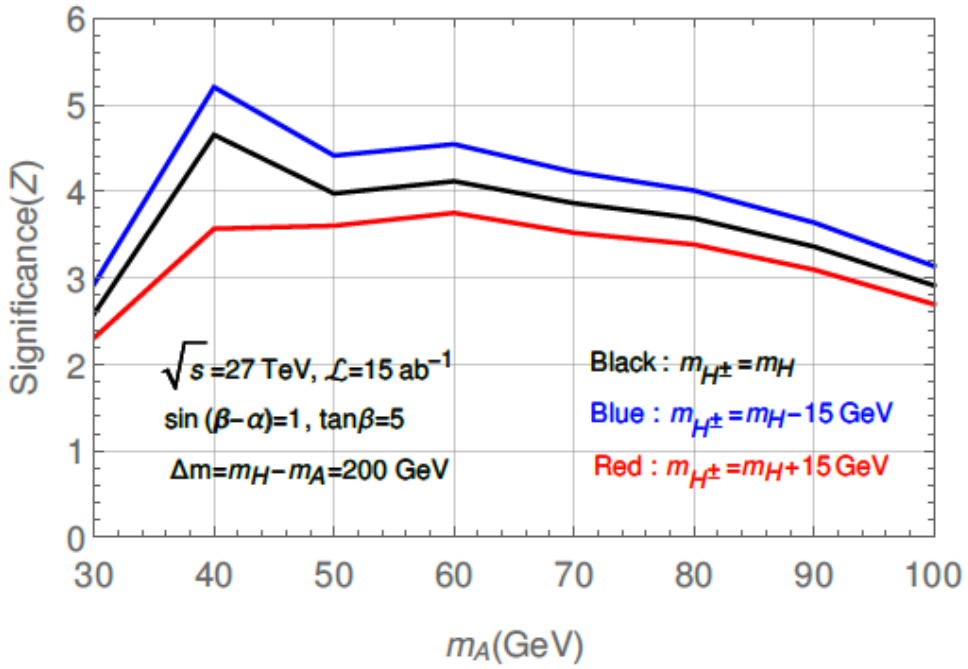

$$M_{bbl^\pm} \leq M_{H^\pm} - 5 \text{ GeV}.$$

$$|M_{bb} - m_A| \leq 15 \text{ GeV}.$$

The significance Z

$$Z = \sqrt{2 \cdot [((s+b) \cdot ln(1+s/b) - s)]}$$

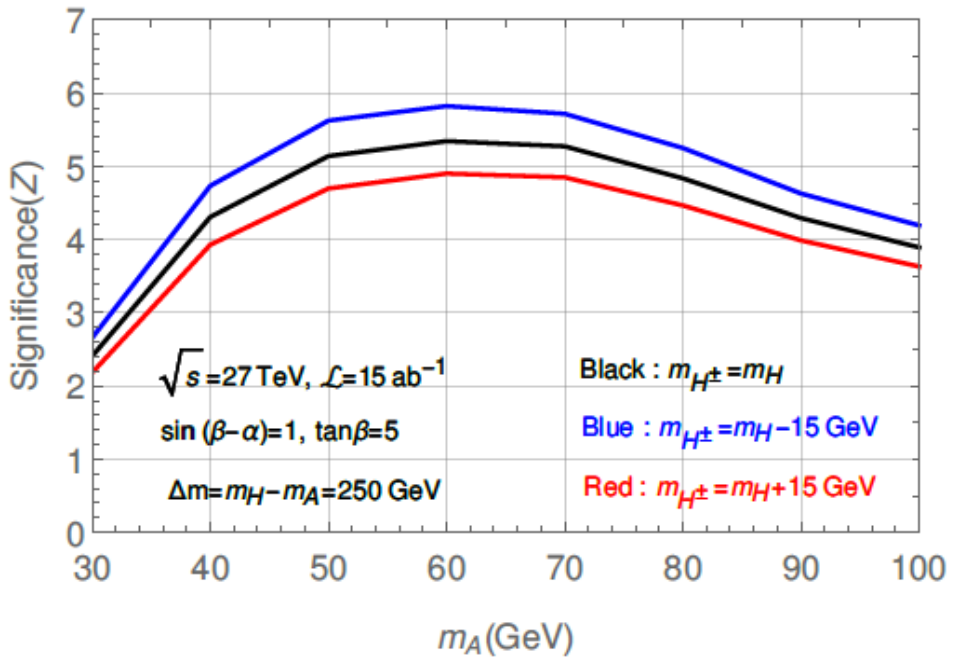

Signal-background analysis for Type-III 2HDM

- The signal process

$$pp \to W^{\pm *}W^{\pm *}j_F j_F \to H^{\pm}H^{\pm}j_F j_F \to (W^{\pm}A^0)(W^{\pm}A^0)j_F j_F \to l^{\pm}\nu(\tau^+\tau^-)l^{\pm}\nu(\tau^+\tau^-)j_F j_F$$

- The main SM backgrounds

$$pp \to t\bar{t}Zjj \to (bW^+)(\bar{b}W^-)(\tau^+\tau^-)jj \to l^{\pm}2b3\tau 2j,$$

$$pp \to t\bar{t}W^{\pm}jj \to (bW^+)(\bar{b}W^-)(\tau^{\pm}\nu_\tau)jj \to l^{\pm}2b2\tau 2j,$$

$$pp \to W^{\pm}W^{\mp}Zjj \to (l^{\pm}\nu_l)(\tau^{\mp}\nu_\tau)(\tau^+\tau^-)jj \to l^{\pm}3\tau 2j,$$

$$pp \to W^{\pm}ZZjj \to (l^{\pm}\nu_l)(\tau^+\tau^-)(\tau^+\tau^-)jj \to l^{\pm}4\tau 2j$$

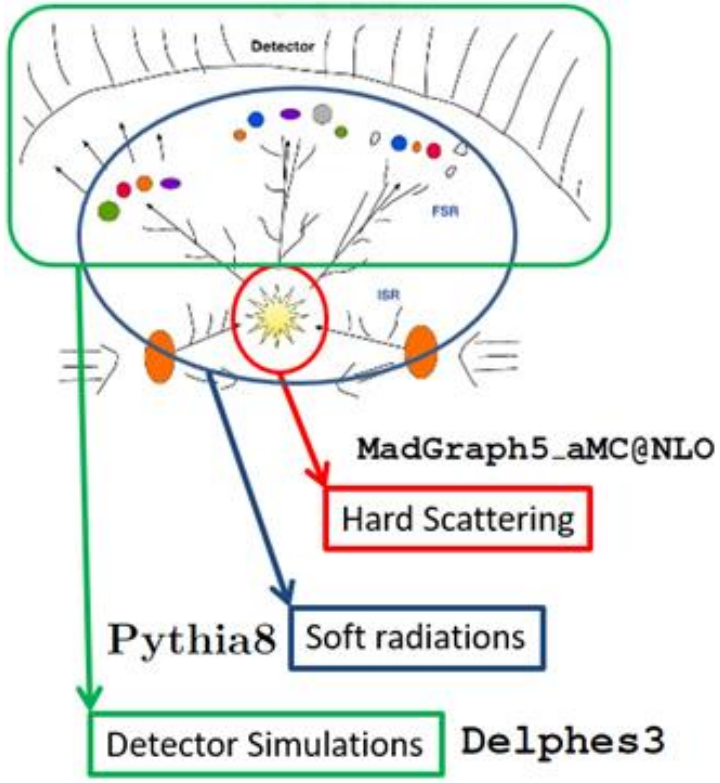

Signal-background analysis for Type-III 2HDM

TABLE VI. Cut flow table for the Type-III 2HDM signal $pp \to H^{\pm}H^{\pm}j_F j_F$ with $m_{H^{\pm}} = 205$ GeV, $m_{A^0} = 65$ GeV, $\Delta m = 200$ GeV, $\tan\beta = 5$ and $\sin(\beta-\alpha) = 0.97$, and various backgrounds at $\sqrt{s} = 14$ TeV.

MadAnalysis5

Cross section (fb)	signal	$t\bar{t}Zjj$	$t\bar{t}W^{\pm}jj$	$W^{\pm}W^{\mp}Zjj$	$W^{\pm}ZZjj$
Preselection	2.98×10^{-2}	3.60×10^{-1}	2.44×10^{-1}	3.28×10^{-2}	1.87×10^{-3}
$N(\tau, l^{\pm}) \geq 3, 2,$ $P_T^{\tau,l^{\pm}} > 20\text{GeV}, \lvert\eta^{\tau,l}\rvert < 2.5$	1.23×10^{-3}	7.42×10^{-3}	1.07×10^{-3}	3.89×10^{-4}	9.61×10^{-5}
$N(j) \geq 2,$ $P_T^j > 30\text{GeV}, M_{jj} > 500\text{GeV}$	9.81×10^{-4}	4.63×10^{-3}	6.19×10^{-4}	1.97×10^{-4}	5.08×10^{-5}
b-jet veto	9.15×10^{-4}	1.15×10^{-3}	2.03×10^{-4}	1.71×10^{-4}	4.32×10^{-5}
$m_{H^{\pm}}$ Cut $M_{\tau^+\tau^-l^{\pm}} < 250\text{GeV}$	8.24×10^{-4}	7.52×10^{-4}	9.18×10^{-5}	1.15×10^{-4}	2.98×10^{-5}
m_{A^0} Cut $40 < M_{\tau^+\tau^-} < 100\text{GeV}$	7.95×10^{-4}	6.28×10^{-4}	5.81×10^{-5}	1.04×10^{-4}	2.73×10^{-5}

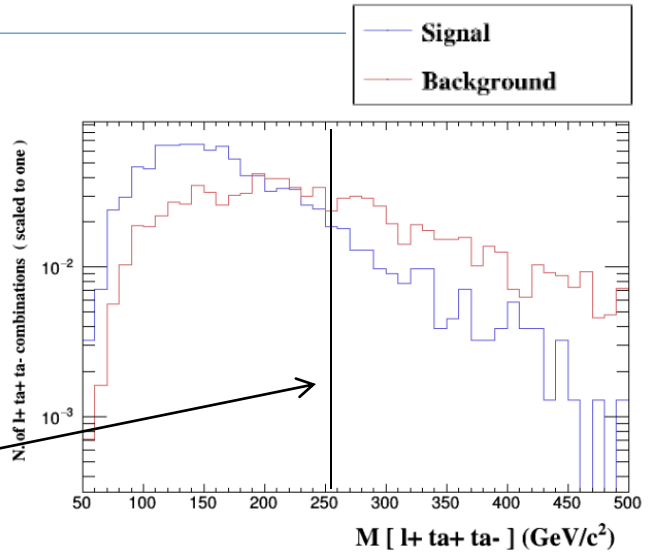

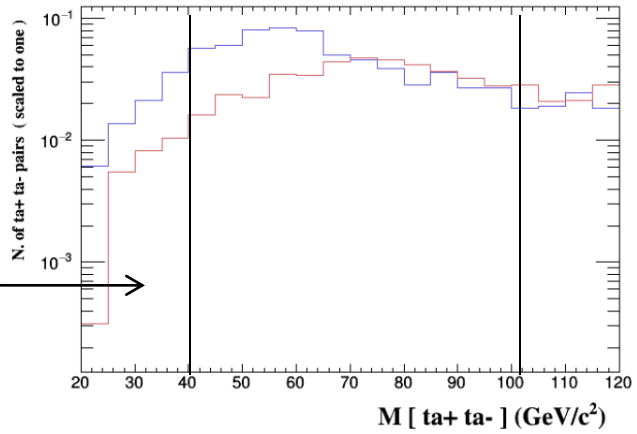

Signal-background analysis for Type-III 2HDM

TABLE VII. Cut flow table for the Type-III 2HDM signal $pp \to H^{\pm}H^{\pm}j_F j_F$ with $m_{H^{\pm}} = 205$ GeV, $m_{A^0} = 65$ GeV, $\Delta m = 200$ GeV, $\tan\beta = 5$ and $\sin(\beta - \alpha) = 0.97$, and various backgrounds at $\sqrt{s} = 27$ TeV.

MadAnalysis5

Cross section (fb)	signal	$t\bar{t}Zjj$	$t\bar{t}W^{\pm}jj$	$W^{\pm}W^{\mp}Zjj$	$W^{\pm}ZZjj$
Preselection	9.93×10^{-2}	2.51	1.49	1.51×10^{-1}	8.62×10^{-3}
$N(\tau, l^{\pm}) \geq 3, 2,$ $P_T^{\tau,l^{\pm}} > 20\text{GeV}, \lvert\eta^{\tau,l}\rvert < 2.5$	4.27×10^{-3}	4.96×10^{-2}	6.14×10^{-3}	1.71×10^{-3}	4.04×10^{-4}
$N(j) \geq 2,$ $P_T^j > 30\text{GeV}, M_{jj} > 500\text{GeV}$	3.71×10^{-3}	3.69×10^{-2}	4.50×10^{-3}	1.08×10^{-3}	2.67×10^{-4}
b-jet veto	3.40×10^{-3}	9.23×10^{-3}	1.41×10^{-3}	9.23×10^{-4}	2.19×10^{-4}
$m_{H^{\pm}}$ Cut $M_{\tau^+\tau^-l^{\pm}} < 200\text{GeV}$	2.75×10^{-3}	4.04×10^{-3}	4.17×10^{-4}	3.94×10^{-4}	1.09×10^{-4}
m_{A^0} Cut $40 < M_{\tau^+\tau^-} < 70\text{GeV}$	2.35×10^{-3}	2.20×10^{-3}	1.96×10^{-4}	2.29×10^{-4}	6.63×10^{-5}

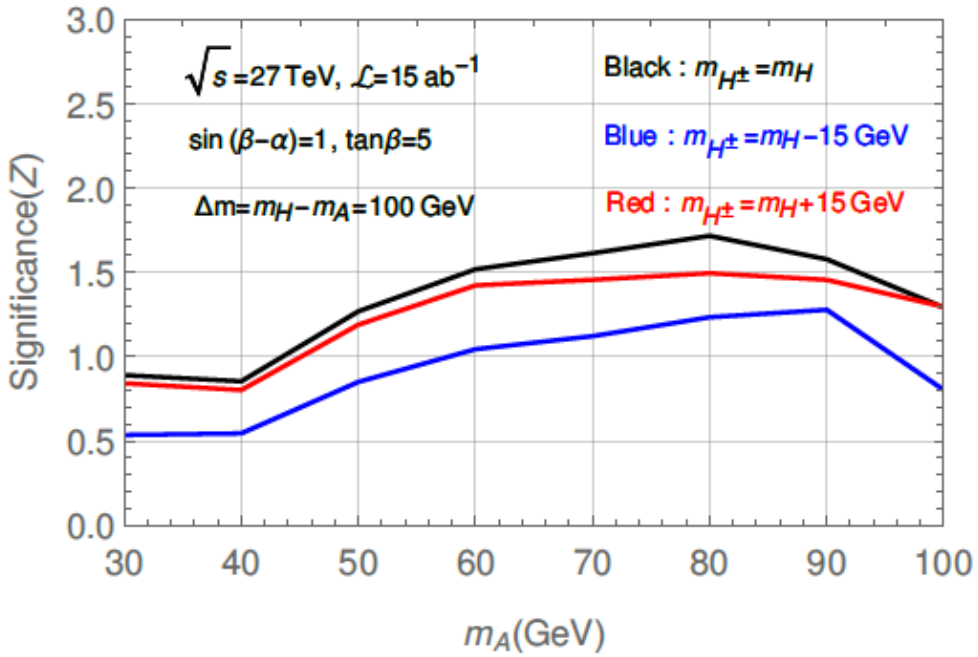

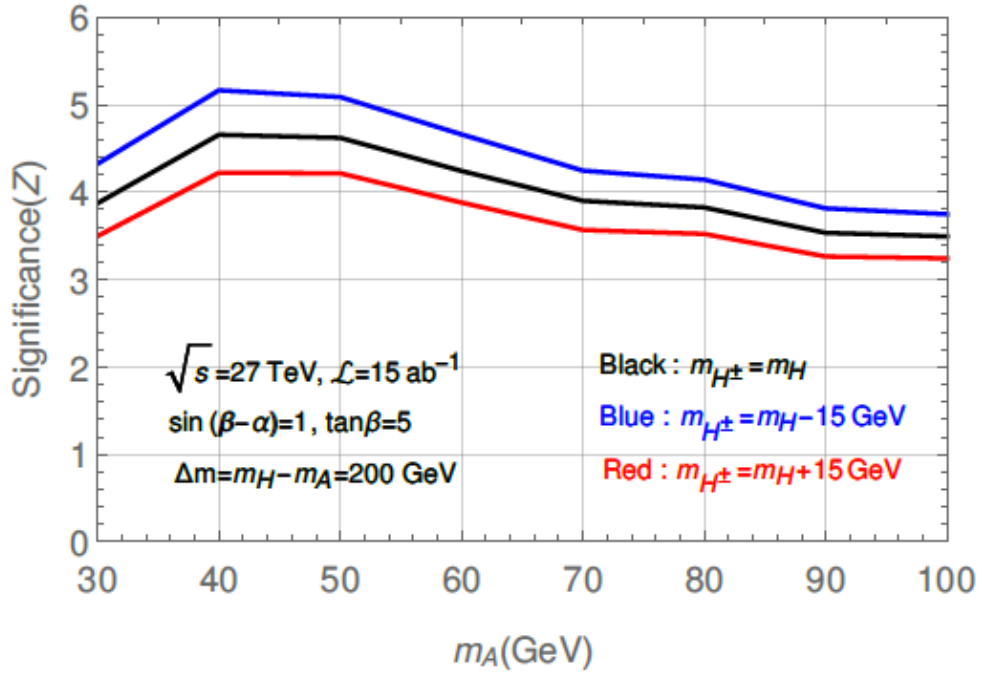

$$M_{\tau^+\tau^- l^\pm} \leq M_{H^\pm} - 5 \text{ GeV}.$$

$$m_{A^0} - 25 \text{ GeV} \leq M_{\tau^+\tau^-} \leq m_{A^0} + 5 \text{ GeV}.$$

The significance Z

$$Z = \sqrt{2 \cdot [((s+b) \cdot ln(1+s/b) - s)]}$$

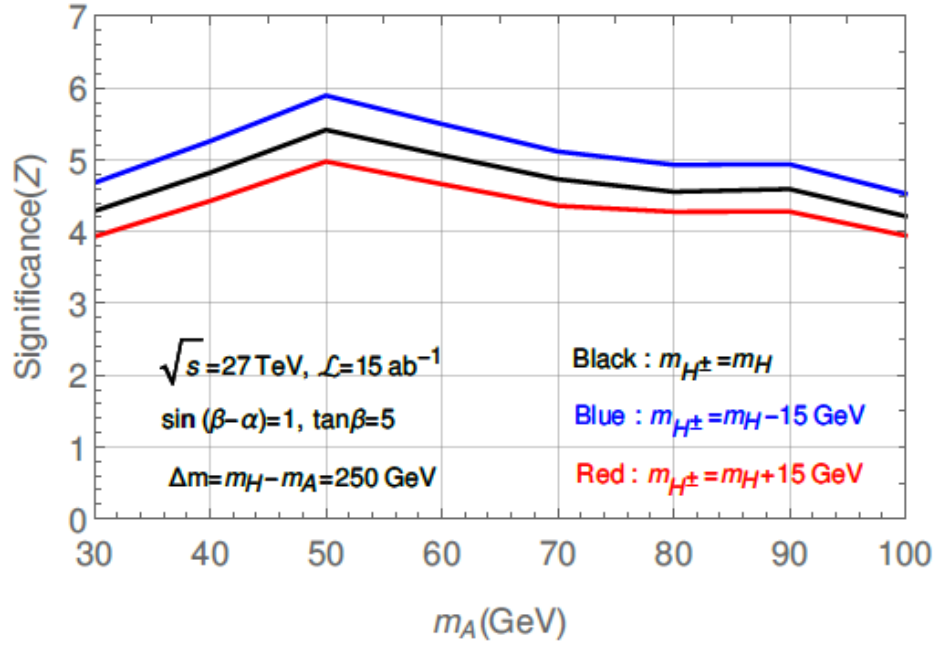

Contents

- 1. Motivation
- 2. Brief review of 2HDM's
- 3. Constraints on 2HDM's
- 4. Same-sign charged Higgs pair production
- **5. Conclusions**

Conclusions

- The 2HDM is one of the most popular extended Higgs sector with rich phenomenology.
- Exploring the whole mass spectrum in 2HDM can help us understand the mystery of EWSB.
- We have studied a novel process - production of same-sign charged Higgs production.

$$pp \to W^{\pm *} W^{\pm *} \to jj H^{\pm} H^{\pm} \to jj (W^{\pm} A^0)(W^{\pm} A^0)$$

- It allows one to probe the whole mass spectrum in the 2HDM for some specific relations.
- We have investigated same-sign charged Higgs-boson production via vector-boson-fusion at the HL-LHC and HE-LHC (27 TeV) in Type I and III 2HDM's.

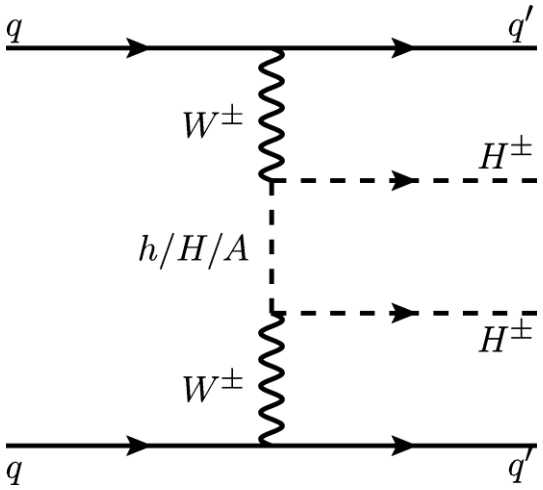

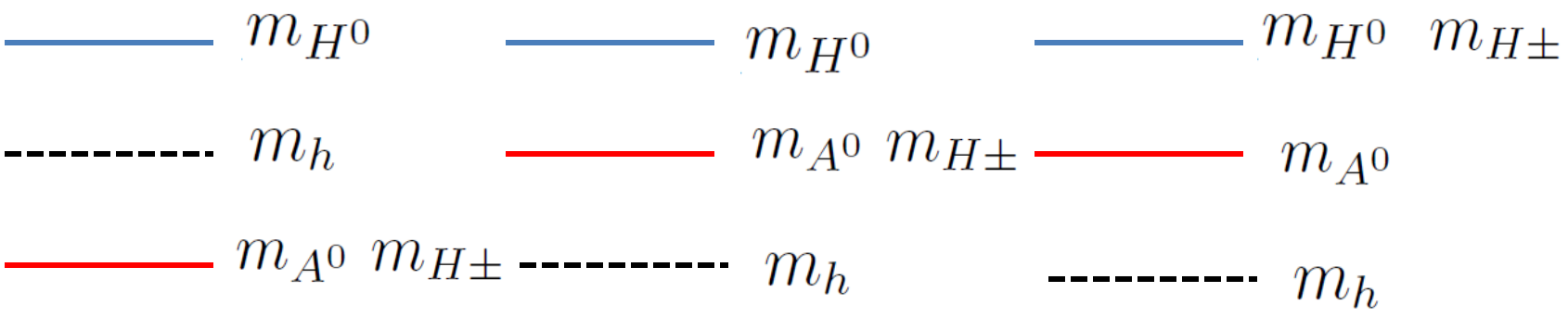

$H^\pm \to \tau\nu \quad H^\pm \to tb$

Masashi Aiko, Shinya Kanemura, Kentarou Mawatari (Osaka U.)

arXiv:1906.09101

Physics Letters B
Volume 797, 10 October 2019, 134854

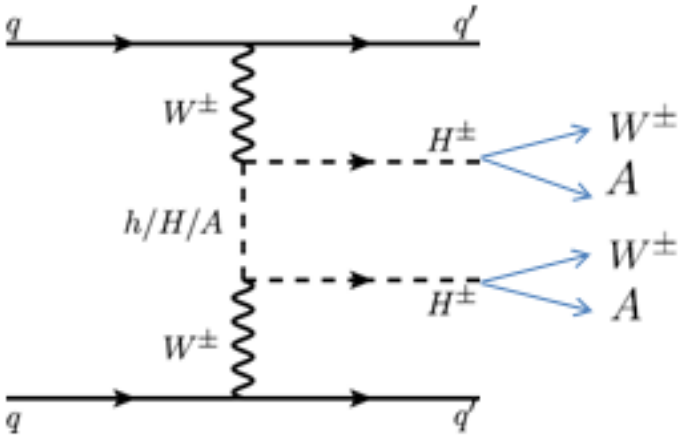

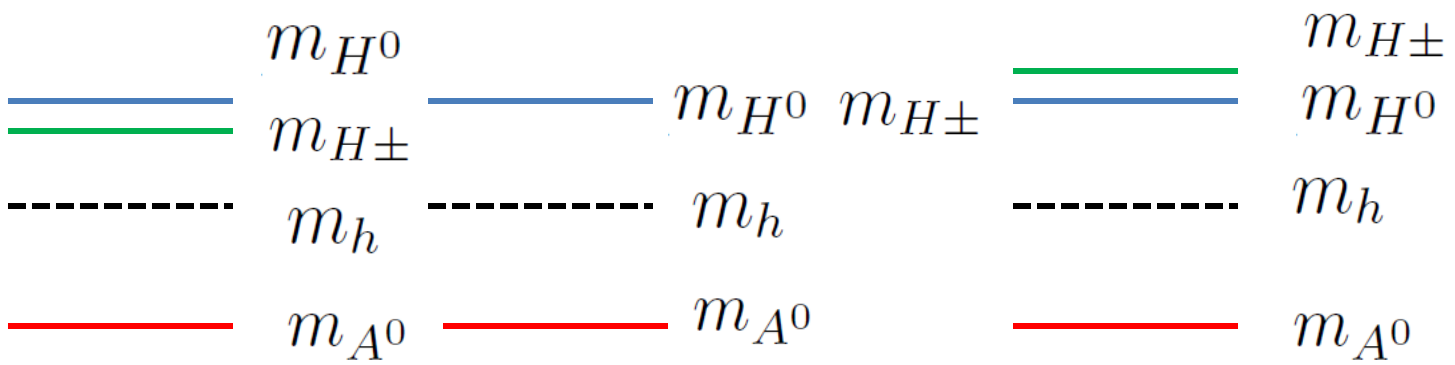

$A^0 \to b\bar{b} \quad A^0 \to \tau\tau$

arXiv:1910.02571

Conclusions

In type I 2HDM, we used the decay channel $H^{\pm}H^{\pm} \to (W^{\pm}A^0)(W^{\pm}A^0) \to (l^{\pm}\nu b\bar{b})\,(l^{\pm}\nu b\bar{b})$ together with a pair of forward jets to perform the signal-background analysis. At the end, we found about 4 signal events versus 5 background events at HL-LHC with luminosity of 3000 fb^{-1} for a typical benchmark point. At the HE-LHC, significance level of $2-5$ can be achieved for $\Delta m = 200 - 250$ GeV.

On the other hand, in type III 2HDM we used the decay channel $H^{\pm}H^{\pm} \to (W^{\pm}A^0)(W^{\pm}A^0) \to (l^{\pm}\nu\tau^{+}\tau^{-})\,(l^{\pm}\nu\tau^{+}\tau^{-})$ together with a pair of forward jets to perform the signal-background analysis. At the HL-LHC, we can achieve the signal-to-background ratio equal to 1, and the number of signal events is about 2 for a luminosity of 3000 fb^{-1}. Nevertheless, at the HE-LHC the significance can rise to the level of $3-6$ for $\Delta m = 200 - 250$ GeV.

Conclusions

In summary, if the mass spectrum in 2HDM has the following relations :

- one light (pseudo)scalar, say A^0,
- a large mass splitting between two neutral scalars, $\Delta m = (m_{H^0} - m_{A^0})$, and
- the charged Higgs mass is above the $W^{\pm}A^0$ threshold,

then we can make use of same-sign charged Higgs-boson production to pin down or rule out this scenario in the near future.

Thank you
for your attention

경청해 주셨어 감사합니다

Back-up Slide

Masashi Aiko, Shinya Kanemura, Kentarou Mawatari (Osaka U.)

arXiv:1906.09101

Physics Letters B

Volume 797, 10 October 2019, 134854

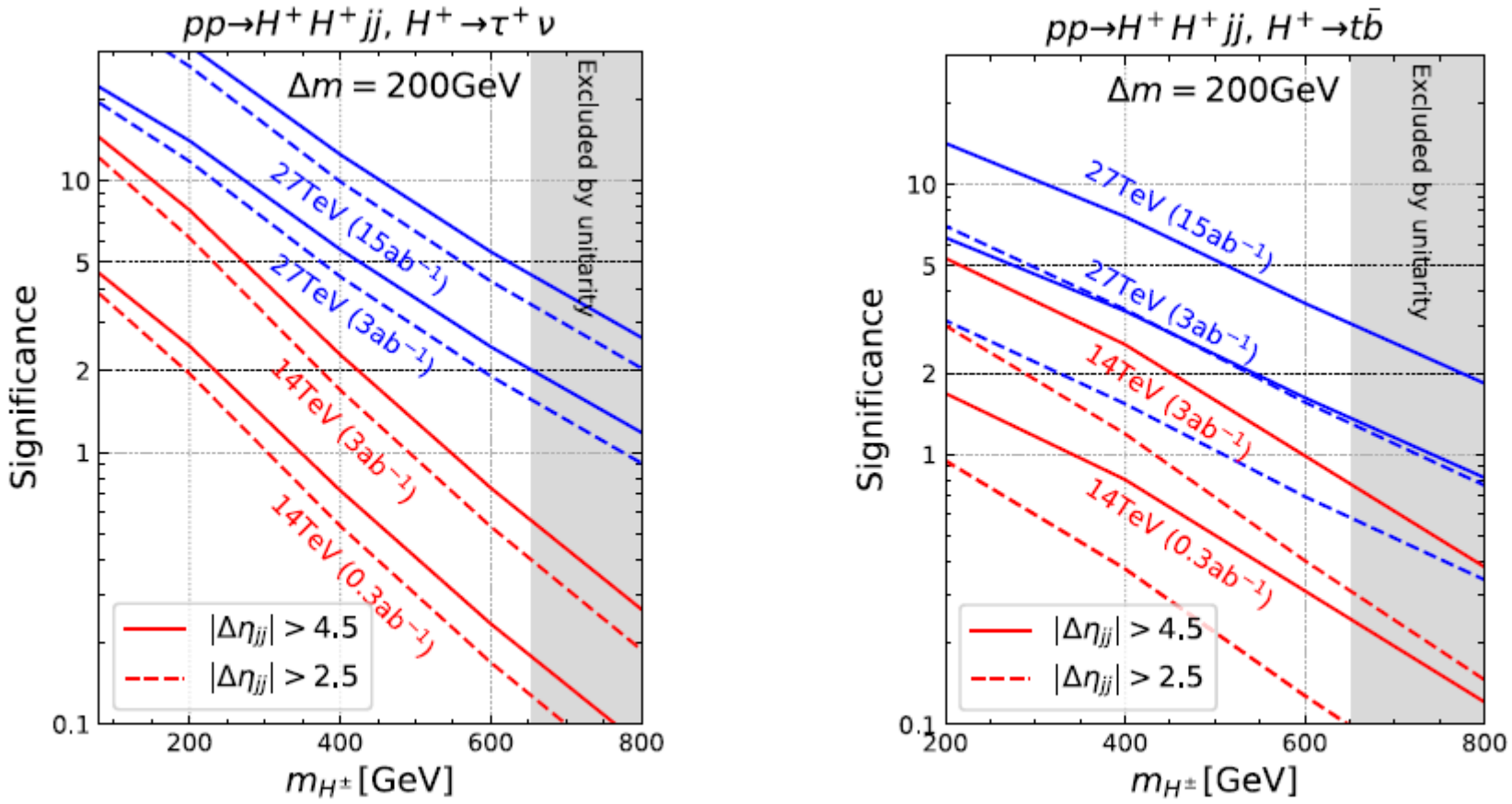

Fig. 3. Signal significance of $pp \to H^+H^+jj$ for $H^+ \to \tau^+\nu$ (left) and $H^+ \to t\bar{b}$ (right).